

Low-temperature structure and phase transitions at the Au/Si (100) interface

Z. Ma and L. H. Allen

Department of Materials Science and Engineering and Coordinated Science Laboratory, University of Illinois, Urbana, Illinois 61801
(Received 22 September 1993)

High-resolution transmission electron microscopy coupled with a STEM nanoprobe reveals that the Au/Si (100) interface deposited at $\sim 80^\circ\text{C}$ is not abrupt and contains a disordered Si-rich Au-Si alloy decorated with pure Au nanocrystallites. The presence of oxygen at the Au surface enhances the outdiffusion of Si atoms through the Au overlayer, resulting in the phase transition from a disordered interface to an ordered metastable Au_4Si phase. Instead, the Au/Si (100) capped with a Ge layer shows that the amorphous structure remains relatively stable. These results allow explanations of some unresolved experimental enigmas.

The interface formed between metal and silicon is critical in determining its ultimate electronic properties. An atomistic view of the interface structure resulting from the deposition of metal atoms on the elemental semiconducting substrates is an important step towards a fundamental understanding of the chemical nature and electronic structure of the interfaces of these technologically vital systems. The Au/Si interface has been a model system for investigating the Schottky barrier formation¹⁻³ as well as the nature of *p-d* hybridization process.⁴ Recently, it has also been used to study the subsurface interface electronic structure by ballistic electron emission microscopy.^{2,3} However, for such an important system, the interface structure is still not clearly resolved and some controversy remains regarding the detailed characteristics of the interface. Many previous experiments^{5,6,10} indicate that the Au/Si (111) interface grown at room temperature is fairly diffuse, containing an intermixed Au-Si alloy. In contrast to this diffuse interface model, some others⁷ suggest that the room-temperature-grown interface is abrupt with the contact made by metallic Au and bulk Si. Since these interface structures are mostly deduced from the results obtained using conventional surface-sensitive techniques, the information achieved is rather limited due to the poor spatial resolution and finite electron escape depth associated with these surface methods. Although of higher technological importance, the Au/Si (100) interface formation is much less investigated.^{8,9} A detailed knowledge of the interface structure is apparently of significant value in order to clarify this controversial issue and to correlate the electronic properties with the interface structure. In this respect, high-resolution transmission electron microscopy (HRTEM) coupling with a scanning transmission electron microscope (STEM) nanoprobe is capable of probing the interface structure on the atomic scale. With these techniques, the exact interfacial structure and its chemical composition can be obtained simultaneously.

One of the most striking consequences of the Au/Si interface formation is the Au-induced breaking of the underlying Si bonds, which catalyzes Si outdiffusion through the Au overlayer and subsequent formation of silicon oxide on the top Au surface while being exposed

in an oxidizing ambient even at room temperature. This oxidation phenomenon has been explored from several different aspects.¹¹⁻¹³ It has been shown that the oxidation process is different than the typical oxidation process of an exposed Si surface which proceeds indefinitely during exposure to an oxidizing ambient. The amount of silicon oxide formed in the Au/Si system seems limited by some intrinsic constraint within the initial Au/Si sample. Although attempts have been made to explain these experimental data, convincing evidence has never been provided. Here, we show that a study of interface evolution could be related to these experimental enigmas and thus leads to a simple convincing explanation.

In this paper, we present a detailed characterization of the Au/Si (100) interface formed at $\sim 80^\circ\text{C}$ using HRTEM coupled with a STEM nanoprobe. The Au/Si (100) interface is found to be diffuse, having a disordered Si-rich Au-Si alloy embedded with pure Au nanocrystallites. The deposition temperature has a dramatic effect on the amorphous alloy formation. We also report studies on the interface evolution of Au/Si (100) structure with and without a Ge capping layer during room-temperature air exposure. These results are discussed by comparing with Au/Si (111) interface and can be reconciled with different spectroscopic data obtained from Au/Si (100) and Au/Si (111) interfaces. Studies of the Au/Si (100) interface evolution lead to our explanation of the limited oxide growth phenomenon.

(100)-oriented Si wafers were first cleaned in organic solvents and then dipped in a dilute HF solution (10:1) prior to loading into an *e*-beam evaporator with a base pressure of 6×10^{-8} Torr. Here, we used a thick Au layer (1400–3500 Å) to bury the interface structure, thus an intact interface structure formed during deposition can be preserved. Au films were deposited onto the Si (100) substrate at both room temperature and $\sim 80^\circ\text{C}$ at a rate of 20 Å/sec to study the effect of deposition temperature on the interface formation. Another Au/Si (100) sample with a Ge capping layer (about 500 Å) was also prepared at $\sim 80^\circ\text{C}$ to address the effect of ambient on the interface evolution. The Ge capping layer used here is intended to act as a diffusion barrier for oxygen indiffusion. The substrate temperature was controlled to within

$\pm 2^\circ\text{C}$. The pressure was maintained below 3×10^{-7} Torr during deposition. The samples were divided into several sets. One set of samples was examined immediately for interfacial structure formed during deposition. The rest were exposed to air at room temperature for different periods of time to allow the oxidation process to occur. Characterization of the interface evolution was carried out on samples deposited at $\sim 80^\circ\text{C}$ by cross-sectional transmission electron microscopy (cross-sectional TEM) and transmission electron diffraction. TEM specimens were prepared by mechanical thinning down to $\sim 30 \mu\text{m}$ followed by cold-stage (liquid- N_2 trap) ion-milling to electron transparency, with special caution to minimizing any heating effects. High-resolution TEM observations were carried out in a Philips CM12 microscope operating at 120 kV. Chemical analysis was performed using a VG-HB5 STEM equipped with a 10-Å nanoprobe. Auger electron spectroscopy (AES) was used to monitor the surface oxide formation.

Figure 1(a) shows the interfacial structure of Au/Si (100) deposited at room temperature. As seen in the micrograph, room-temperature deposition of Au onto Si (100) induced a disordered layer of about 15 Å thick (indicated by arrows, denoted by a label *a* in the figure). The amorphous layer was nonuniformly formed between pure Au and underlying Si substrate, suggesting possible presence of impurities on a HF-treated Si surface. Figure 1(b) shows the interface structure formed during Au deposition at $\sim 80^\circ\text{C}$. In this case, a much thicker amorphous layer (about 80 Å on the average) is observed. The Si atoms are disrupted from the Si substrate due to the deposition of Au, resulting in a very diffuse transition be-

tween the amorphous layer and Si. The transition between amorphous layer and pure Au appears relatively abrupt. Fine features in the amorphous layer are well delineated by the revealing contrast. In order to fully identify the amorphous layer, we have employed a STEM nanoprobe, which is able to obtain structure information from features on the order of 20 Å and also to determine its local composition over ~ 50 Å (effective probe size). Figures 1(c) and 1(d) show typical electron nanodiffraction patterns obtained from the particlelike features inside the amorphous layer. These patterns match very well with [100] and [112] zone axis patterns of single-crystal Au. This indicates that the particles embedded in the amorphous layer are pure Au nanocrystallites. The average size of the Au particles is about 25 Å. It is also noticed, in this and other images, that there are Au particles in close proximity to the Si substrate. The average composition of the amorphous layer is approximately $\text{Au}_{0.40}\text{Si}_{0.60}$. The composition variations of this layer cannot be measured due to the limitation of effective size of the probe. By combining HRTEM results with STEM analysis, the Au/Si (100) interface formed at $\sim 80^\circ\text{C}$ can be depicted to contain a Si-rich Au-Si amorphous alloy with pure Au nanocrystallites embedded in it.

In agreement with previous experiments,^{11,13} after the Au/Si (100) being exposed to atmospheric ambient at room temperature for ~ 60 days, some brownish color was observed on the Au surface. AES analysis reveals the existence of both Si and O on the surface and the position of Si (*LVV*) peak being shifted to 76 eV. This clearly indicates that a surface SiO_x layer has formed. In comparison, the sample capped with a Ge layer did not exhibit any visible color change at the surface. To correlate surface oxide formation with evolution of the buried interface, we analyzed both samples deposited at $\sim 80^\circ\text{C}$ with and without a Ge capping layer using cross-sectional TEM. Figure 2(a) shows a typical interface structure for a Au/Si (100) sample at this stage. It is clearly seen that except for slight increase in the thickness of the amorphous layer, some crystalline precipitates formed at the interface between amorphous alloy and Si substrate. A typical selected area electron diffraction pattern is also presented in Fig. 2(b). We performed an analysis on selected area diffraction patterns obtained from different areas along the interface as well as dark-field imaging on the precipitates. The results indicate that these crystalline precipitates can be assigned to metastable Au_4Si phases¹⁴ [denoted by subscript *p* in Fig. 2(b)]. STEM measurement also shows that the average composition of the amorphous alloy becomes slightly Au-enriched, indicating that the outdiffusion of Si atoms has occurred. The Ge-capped Au/Si (100) does not show any noticeable change in interfacial structure. In this case, the amorphous alloy developed during Au deposition is relatively stable.

Further exposure to air resulted in the growth of surface silicon oxide in the case of Au/Si (100), as revealed by AES depth profile. We found that corresponding to a further growth of surface oxide, the amorphous alloy gradually transformed to the metastable Au_4Si phase.

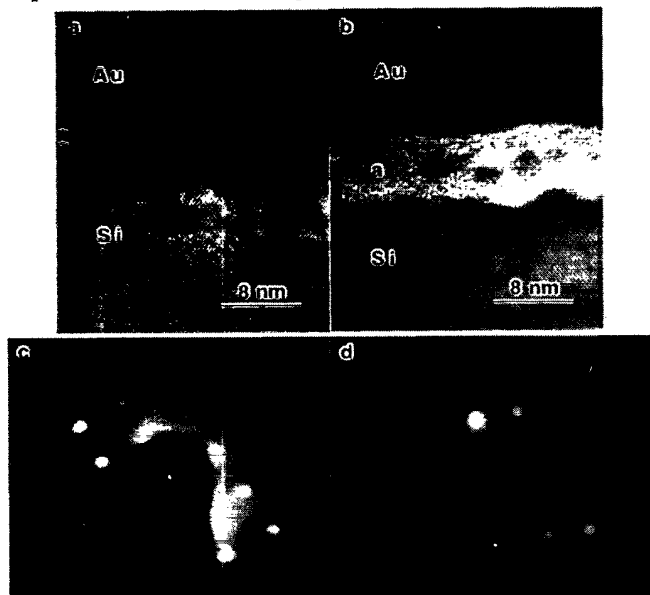


FIG. 1. High-resolution TEM images of Au/Si (100) interface deposited at (a) room temperature and (b) about 80°C . The samples were viewed along the [110] axis. Label *a* represents an amorphous Au-Si alloy. The particles observed in the alloy are identified in (c) and (d). Typical electron diffraction patterns obtained using a STEM nanoprobe from the particles embedded in the amorphous alloy, matching very well with fcc Au (c) [100], and (d) [112] zone axis patterns.

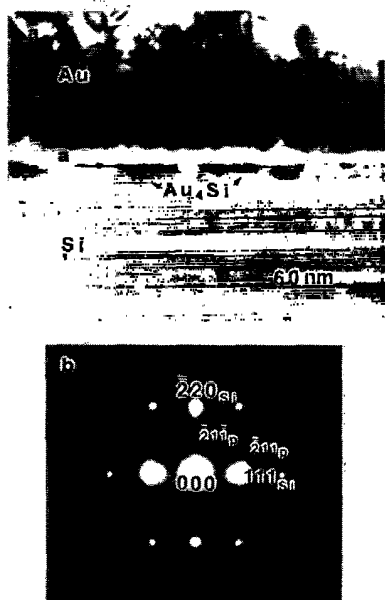


FIG. 2. (a) Cross-sectional TEM image of the Au/Si (100) interface deposited at $\sim 80^\circ\text{C}$ and after room-temperature air exposure for 60 days. Label *a* represents an amorphous Au-Si alloy. The Au_4Si precipitates are observed at the Si interface. (b). A typical selected area diffraction pattern taken from the interface area, showing orientation relationships between Au_4Si phase (denoted by a subscript *p* here) and Si substrate.

This transition proceeds in a nonuniform manner, i.e., the transition in some places appears faster than in other places. This nonuniform interface behavior resulted in the nonuniform formation of silicon oxide on the Au surface. At the same time, no structural changes were observed at the Au/Si (100) interface for a Ge-capped sample. Figure 3 shows the interface structure for Au/Si (100) after air exposure for about 150 days. The amorphous Au-Si alloy was completely replaced by a polycrystalline Au_4Si phase (or a mixture of Au_4Si and Au). About 200-Å-thick silicon oxide on average was formed on the surface of Au, as found by both cross-sectional TEM and AES depth profiling. Prolonged exposure does not result in further change of the interface structure as well as substantial increase of the oxide thickness, indicating that the surface oxide probably reaches its limiting thickness.

Our results demonstrate that the deposition temperature has a dramatic effect on the extent of Au/Si (100) interface intermixing reaction. This point is usually not made clear in previous studies on Au-catalyzed silicon oxidation where a link between the thickness of the oxide and amorphous alloy can be found.^{12,13} Also, this kind of quantitative information could not be established by surface science studies due to the limited electron escape depth.

The extensive work on Au/Si interface formation was initially stimulated by the surprising experimental finding of Au-catalyzed room-temperature silicon oxide formation.¹¹ The main objective of these researches was to understand the initiation of Au-induced Si bond breaking.^{5,6,10,15-17} AES studies reveal the formation of Au-Si

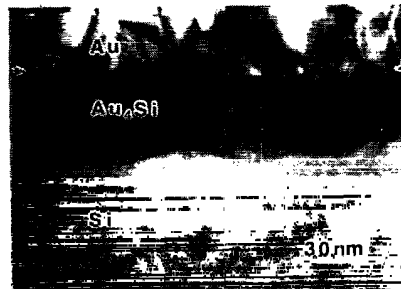


FIG. 3. Interfacial structure of Au/Si (100) deposited at $\sim 80^\circ\text{C}$ and after 150-day air exposure at room temperature. The amorphous Au-Si alloy was completely replaced by a polycrystalline Au_4Si phase. The arrows show the original interface between pure Au and amorphous alloy.

bond through an alloyed amorphous phase based upon the observation of the splitting of the Si (*L*VV) line into a doublet at 90 and 95 eV. This splitting reflects the modification of the Si 3*p* states upon hybridization with the Au 5*d* valence states.^{8,9,17} Our structure determination of the Au/Si (100) interface points out not only the formation of Au-Si amorphous alloy but also the existence of Au clusters in the alloy. This difference can be readily resolved by knowing the fact that the Auger Si (*L*VV) peak is very sensitive to the *p* electronic states of Si atoms and therefore to the bond formation in the Au-Si alloy, but the Au (*N*VV) peak is not modified by the alloying and thus cannot distinguish between pure Au and Au-Si alloy. As mentioned earlier, Au/Si (100) interface formation has been less studied, mainly by low-energy electron diffraction, AES, and transmission channeling.^{8,9} Instead, Au/Si (111) interface was extensively investigated using a variety of surface techniques. In these studies, AES analysis only reveals the same Si (*L*VV) splitting as in the Au/Si (100) case, but high-resolution electron energy-loss spectroscopy and ultraviolet photoemission spectroscopy data clearly indicate that the Au clusters should be grown in the Au-Si alloy. The discrepancy can be readily clarified by the simultaneous presence of pure Au and Au-Si alloy established from our results. This clearly demonstrates that a detailed knowledge of the interface structure could play an essential role in interpreting and understanding its electronic behavior. It is also implied from these studies that the low-temperature behavior of the interface formation is very similar between Au/Si (100) and Au/Si (111) systems.

Our studies on the Au/Si (100) interface evolution indicate that an oxidizing ambient such as air used in this work can greatly enhance the Si outdiffusion toward the surface in the absence of a Ge capping layer, resulting in the surface oxide growth and the phase transition from an amorphous alloy to a crystalline phase. The microstructure analysis of the interface for samples after different degrees of ambient exposure reveal that, as Si atoms outdiffuse to the surface, the amorphous alloy becomes Au-enriched and the gold silicide precipitates start to form. The cause of this transition is believed to be triggered by the extensive outdiffusion of Si atoms due to the presence of oxygen on the Au surface. This argument

is supported by the observation of relatively stable Au-Si alloy in the Ge-capped sample where the Si outdiffusion is suppressed by the presence of the Ge cap. It is conceivable that the thickness of deposited Au film will affect the kinetics of the Si outgoing and thus the phase transition at the interface. From a thermodynamic viewpoint (see Fig. 4), the Au-Si amorphous alloy formed during deposition is highly metastable with an initial composition range of ΔC_{eq} . The Si outdiffusion causes this amorphous layer to be increasingly richer in Au. As the Au concentration exceeds point *a*, it becomes thermodynamically unstable. The crystalline Au_4Si metastable phase will start to form. Thus, the instability of the amorphous alloy is enhanced by the loss of Si within this layer. The subsequent phase transition is thermodynamically favorable.

Based upon our experimental results, the limited oxide growth enigma is explained as follows: the formation of amorphous Au-Si alloy during Au deposition provides metallicly bonded Si atoms through the hybridization of Si 3*p* and Au 5*d* states. These Si atoms are easily released and diffuse out to the surface in the presence of oxygen due to modified surface potential.¹⁸ The outdiffusion of Si enhances the instability of the amorphous alloy, resulting in the gradual phase transition from a Au-Si amorphous alloy to a crystalline Au_4Si phase. This structural change alters the Si bonding environment and thus suppresses or even terminates the further release of Si atoms at low temperature, being the main reason for a limited thickness formation of silicon oxide on the surface. Apparently, this work offers satisfactory explanations for numerous previous results on this issue.¹¹⁻¹³

In conclusion, we find that the Au/Si (100) interface deposited at $\sim 80^\circ C$ is not abrupt and contains a Si-rich Au-Si amorphous alloy decorated with pure Au nanoparticles. The deposition temperature has a large effect on the extent of the amorphous alloy formation. These results provide a detailed picture of the Au/Si (100) inter-

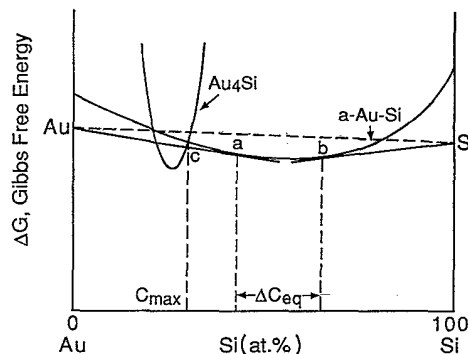


FIG. 4. Schematic Gibbs free energy vs composition curve, showing the relative stability of the amorphous Au-Si alloy and the crystalline Au_4Si metastable phase. The ΔC_{eq} represents the composition range of the amorphous alloy established by the local equilibria. Point *c* represents the maximum Au concentration the alloy could reach before transforming to the Au_4Si phase.

face structure and can be correlated with their electronic properties. During room-temperature ambient exposure, the Au/Si (100) interface gradually transformed from the Au-Si amorphous alloy to the crystalline Au_4Si phase, being triggered by oxygen-enhanced Si outdiffusion. The onset of this phase transition is explained using a thermodynamic model. In comparison, the amorphous alloy in a Ge-capped Au/Si (100) remains relatively stable. The data allow a simple explanation of the limited oxide growth enigma.

We would like to acknowledge the support from the Joint Services Electronics Program (JSEP) under Contract No. N00014-90-J-1270 and from Petroleum Research Fund Grant No. ACS-PRF#25422-G5. We are also grateful to J. M. Gibson for his critical reading of the manuscript. Materials characterization was carried out in the Center for Microanalysis of Materials at the University of Illinois.

¹For an excellent review, see A. Cros and P. Muret, *Mater. Sci. Rep.* **8**, 271 (1992).

²W. J. Kaiser and L. D. Bell, *Phys. Rev. Lett.* **60**, 1406 (1988).

³L. D. Bell and W. J. Kaiser, *Phys. Rev. Lett.* **61**, 2368 (1988).

⁴S. L. Molodtsov, C. Laubschat, G. Kaindl, A. M. Shikin, and V. K. Adamchuk, *Phys. Rev. B* **44**, 8850 (1991).

⁵L. Braicovich, C. M. Garner, P. R. Skeath, C. Y. Su, P. W. Chye, I. Lindau, and W. E. Spicer, *Phys. Rev. B* **20**, 5131 (1979).

⁶P. Perfetti, S. Nannarone, F. Patella, C. Quaresima, M. Capozzi, A. Savoia, and G. Ottaviani, *Phys. Rev. B* **26**, 1125 (1982).

⁷J. J. Yeh, J. Hwang, K. Bertness, D. J. Friedman, R. Cao, and I. Lindau, *Phys. Rev. Lett.* **70**, 3768 (1993).

⁸H. S. Jin, T. Ito, and W. M. Gibson, *J. Vac. Sci. Technol. A* **3**, 942 (1985).

⁹M. Hanbucken, Z. Imam, J. J. Metois, and G. Le Lay, *Surf. Sci.* **162**, 628 (1985).

¹⁰G. Mathieu, R. Contini, J. M. Layet, P. Mathiez, and S. Giorgio, *J. Vac. Sci. Technol. A* **6**, 2904 (1988).

¹¹A. Hiraki, F. Lugujo, and J. W. Mayer, *J. Appl. Phys.* **43**, 3643 (1972).

¹²C. A. Chang and G. Ottaviani, *Appl. Phys. Lett.* **44**, 901 (1984).

¹³A. A. Pasa, H. Paes, Jr., and W. Losch, *J. Vac. Sci. Technol. A* **10**, 374 (1992).

¹⁴L. Hultman, A. Robertsson, H. T. G. Hentzell, I. Engstrom, and P. A. Psaras, *J. Appl. Phys.* **62**, 3647 (1987).

¹⁵A. Hiraki, *J. Electrochem. Soc.* **127**, 2662 (1980).

¹⁶M. Iwami, T. Terada, H. Tochihiro, M. Kubota, and Y. Murata, *Surf. Sci.* **194**, 115 (1988).

¹⁷H. Dallaporta and A. Cros, *Surf. Sci.* **178**, 64 (1986).

¹⁸C. A. Chang, *J. Electrochem. Soc.* **127**, 1331 (1980).